Препринти Інституту фізики конденсованих систем НАН України розповсюджуються серед наукових та інформаційних установ. Вони також доступні по електронній комп'ютерній мережі на WWW-сервері інституту за адресою http://www.icmp.lviv.ua/

The preprints of the Institute for Condensed Matter Physics of the National Academy of Sciences of Ukraine are distributed to scientific and informational institutions. They also are available by computer network from Institute's WWW server (http://www.icmp.lviv.ua/)

Ігор Васильович Стасюк
Володимир Олександрович Краснов

Модель Бозе-Фермі-Хаббарда в границі важких ферміонів

Роботу отримано 26 грудня 2014 р.

Затверджено до друку Вченою радою ІФКС НАН України

Рекомендовано до друку відділом квантової статистики

Виготовлено при ІФКС НАН України

Національна академія наук України

ІНСТИТУТ
ФІЗИКИ
КОНДЕНСОВАНИХ
СИСТЕМ

ICMP–14–08E

I.V. Stasyuk, V.O. Krasnov

BOSE-FERMI-HUBBARD MODEL IN THE HEAVY FERMION LIMIT

ЛЬВІВ

УДК: 538.945

PACS: 71.10.Fd, 71.38

Модель Бозе-Фермі-Хаббарда в границі важких ферміонів

І.В. Стасюк, В.О. Краснов

Анотація. Досліджено фазові переходи в моделі Бозе-Фермі-Хаббарда в наближенні середнього поля та жорстких бозонів при врахуванні одновузлової бозон-ферміонної взаємодії типу відштовхування та у випадку безмежно малого переносу ферміонів. Проаналізовано поведінку параметра порядку бозе-конденсату та термодинамічного потенціалу як функцій хімічного потенціалу бозонів. Встановлено можливість зміни роду фазового переходу до надплинної фази у певних областях значень хімічних потенціалів бозе- та фермі-частинок. У випадках $T = 0$ та $T \neq 0$ побудовано відповідні фазові діаграми на площині (температура, хімічний потенціал бозонів) при різних значеннях параметра переносу бозонів та хімічного потенціалу ферміонів μ'.

Bose-Fermi-Hubbard model in the heavy fermion limit

I.V.Stasyuk, V.O.Krasnov

Abstract. The phase transitions in the Bose-Fermi-Hubbard model in the mean field and hard-core boson approximations, in the case of infinitely small fermion transfer and repulsive on-site boson-fermion interaction, are investigated. The behavior of the BE condensate order parameter and grand canonical potential as functions of the chemical potential of bosons is analyzed. The possibility of change of order of the phase transition to the superfluid phase in certain range of the values of the chemical potentials of Bose- and Fermi-particles is established. For the cases $T = 0$ and $T \neq 0$ the phase diagrams in the plane (temperature, boson chemical potential) for different values of parameters of boson transfer and chemical potential of fermions μ' are built.

1. Introduction

Physics of many-particle systems with strong short-range correlations is one of the important research fields. A new outbreak of activity in this area is associated with manifestations of peculiar properties of ultracold atomic systems in traps at imposing periodic field created by the interference of coherent laser beams. In created in a such way optical lattices, in the case of Bose-atoms, transition to the state with Bose-Einstein condensate at very low temperatures ($T < 10^{-7}...10^{-8}K$) occurs. Experimentally, this effect was observed for the first time by Greiner and others in 2002–2003 [1,2] in the system of ^{87}Rb atoms. Bose-Einstein condensation occurs in this case by the phase transition of the 2nd order from the so-called Mott insulator phase (MI-phase) to the superfluid phase (SF-phase). The theoretical description of the phenomenon is based on the Bose-Hubbard model [3,4], which takes into account two main factors that determine the thermodynamics and energy spectrum of the system of Bose-particles – tunneling between neighbour minima of potential in the lattice and short-range on-site repulsive interaction of Hubbard type. A lot of investigations [5-14] are dedicated to the construction of phase diagrams that define the conditions of existence of SF-phase at $T = 0$ and at non-zero temperatures as well as to the study of different aspects of one-particle spectrum (see, also, reviews [15–17]).

Along with ultracold atomic Bose-systems the boson-fermion mixtures in optical atomic lattices are also actively researched. Their experimental implementation (eg, spin-polarized mixtures of $^{87}Rb - ^{40}K$ atoms [18–20]) allowed to see the MI-SF transition in the presence of Fermi-atoms. An important factor, that has been observed, is fading of bosons coherence and the decay of condensate fraction in SF-phase in a certain range of thermodynamic parameter (chemical potential bosons or temperature) values influenced by the interaction with fermions. This is reflected in the change of conditions of existence of SF- and MI- phases and the shift of curve of SF-MI transition on the phase diagram. As a possible explanations of this effect, the renormalization (due to self-trapping) of tunneling hopping of bosons [18,20,21], influence of higher boson bands [22,23], intersite interactions (including so-called correlated hopping) [24] are considered. An important feature of boson-fermion mixtures is the possible existence of new quantum phases such as CDW-type phase (with the particle density modulation), supersolid (SS) phase (with the spatial modulation of the density as well as the order parameter of condensate), SF_f phase (with the condensate of fermion pairs), and their various combinations (see, in particular, [25]). Another interesting factor that must be taken into consideration is the formation of so-called fermion composites [26, 27], which are result of fermion pairing with one or more bosons (or one or more boson holes) due to their effective attraction (or repulsion). Interspecies interaction in this case can be changed [28] using the Feshbach resonance [29]. A characteristic here is the asymmetry between the attraction and repulsion cases in the behavior of boson-fermion mixtures and in the phase diagrams [18, 30].

To describe the boson-fermion mixtures in optical lattices the Bose-Fermi-Hubbard model is used. Model and it's microscopic justification were proposed in [30]. Following this, in [31, 32] the phase diagrams at $T = 0$ (ground state diagrams) in the mean-field approximation were constructed. As well, the ion transfer was taken into account by means of perturbation theory in order to do this; the effective static interaction between bosons (in the cases $J_B = J_F = 0$; $J_B \neq 0, J_F = 0$; $J_B = J_F = J$, where J_B, J_F are the parameters of the ion transfer) was included. An areas of the existence of phases with composite fermions, containing different number of bosons (or boson holes), were found. The analysis was performed in the regime of fixed fermion density.

In [33] as well as in subsequent studies [34, 35], it was shown within the BFH model that the direct boson-fermion interaction can lead to effective dynamic interaction between bosons through fermionic field. This gives the appearance of instability; when $\overrightarrow{q} = 0$ – in regard to phase separation, and when $\overrightarrow{q} = \overrightarrow{k}_{DW}$ – in regard to spatial modulation and SS phase formation (which in the case of half-filling for fermions and the increase of energy of their repulsion off bosons becomes a CDW phase [36]). Mechanisms of arising of SS phase were studied in some other works (see. in particular [25]). Bose-Einstein condensate enhances the s-wave pairing of fermions, while uncondensed bosons are contributing to the appearence of CDW. At half-filling for fermions SF_f-phase competes with antiferromagnetic ordering [37].

On the other hand, at the spin degeneracy, the reverse effect is possible, when pairing of fermions is induced by bosons. This situation is analogous to the formation of Cooper pairs in the BCS model, as was shown in several papers (see, [38–40]). It results in creation of a phase SF_f, where the role of the superfluid component belongs to fermion pairs; corresponding phase diagrams are constructed in [25]. Integration over fermionic variables provides also an additional static interaction between bosons U_{BB}, which promotes $MI \to SF$ transition or suppresses it. To a large extent it depends on the mass ratio of Bose- and Fermi-atoms (on the ratio of hopping parameters t_F/t_B). The phase diagram obtained by functional integration and the Gutzwiller approach in the cases of "light" (a mixture of $^{87}Rb - ^{40}K$ atoms) and "heavy" (a mixture of $^{23}Na - ^{40}K$ atoms) fermions are given in [34].

Another aspects of fermion influence on the $MI \to SF$ phase transition in boson subsystem were investigated in [22–41]. It is shown, in particular, that virtual transitions of bosons under the influence of interaction U_{BF} through their excited states in the optical lattice potential minima lead to extension of the MI phase region at $T = 0$ (the shift of the curve of the phase transition in the (t, μ) plane towards larger values of the t/U ratio). The similar role is played by retardation at the boson screening by fermions and "polaron effect" [42]. It manifests in the reduction of parameter of bosons transfer t_B and their slowing down. However, for heavy fermions the SF phase region in the case of intermediate temperatures broadens [35]. Interparticle interactions, in particular the so-called bond-charge interaction, can have a significant influence on the transfer of bosons as shown in [24]. This also can lead to the shift of transition from MI to SF phase.

A separate direction of theoretical description of boson atoms and boson-fermion mixtures in optical lattices is associated with the use of the hard-core boson approach, where the occupation of on-site states conforms to the Pauli principle. For Bose atoms on the lattice this model is a limiting case of Bose-Hubbard model for $U \to \infty$ and widely enough used [43–47]. It is suitable for the region $0 \leq \overline{n}_B \leq 1$, but also can describe the MI-SF phase transitions in the vicinity of the points $\mu_B = nU, n = 0, 1, 2...$ at finite values of U (in the case of strong coupling, $t_B \ll U$) where $n \leq \overline{n}_B \leq n+1$ for $T = 0$ within the SF phase region [13, 14]. In these cases, the model is applicable also to such phase transitions at non-zero temperatures.

For boson-fermion mixtures the BFH model in hard-core bosons limit remains less explored. In [48] the phase diagrams and phase separation or charge modulation conditions at the ion intercalation in semiconductor crystals were investigated on the basis of BFH-type model; in [49, 50] within pseudospin-fermion description (that corresponds to the mentioned $U \to \infty$ limit) the conditions of of SS and CDW phases appearance under effective interparticle interactions were investigated. For the four-state model, that arises in this case, the calculations for fermion band spectrum in Hubbard-I approximation were performed and its transformation during transition to the SF-phase and at the presence of a Bose-Einstein condensate [51] was investigated.

The aim of this work is a more thorough thermodynamics study of mentioned 4-state model. We confine ourselves to the case of "heavy" fermions (i.e. extremely low values of fermion hopping parameter t_F).

Such a situation was partially considered in [23, 31]. It was argued, in particular, that frozen fermions, as fixed subsystem when $t_F = 0$, can prevent the occurrence of long-range correlations of superfluid-type and appearance of BE condensate. There exists, however, the critical fermion concentration below which this effect is absent (for $d = 2, \overline{n}_p^{crit} \sim 0,59$; for $d = 3, \overline{n}_p^{crit} \sim 0,31$; see [23]).

We consider the equilibrium case, assuming that t_f takes the small values, but not so small that could lead to a state of the glass type [15,52,53]. We will use the mean-field approximation, basing however on accurate allowance for interspecies interaction in the spirit of the strong coupling approach. An analysis of the MI-SF phase transition, based on the conditions of thermodynamic equilibrium, will be performed (we don't restrict ourself to the criterion of the normal (MI) phase stability to determine the phase transition point). The study will be performed in the case of fixed chemical potentials of bosons μ_B and fermions μ_F at $T = 0$, as well as at non-zero temperatures. Corresponding phase diagrams, taking into account the possibility of a change of the phase transition order from the second to the first one, will be built. Our investigation will cover the case of repulsive on-site interaction between hard-core bosons and fermions ($U_{BF} > 0$).

2. Hamiltonian of the BFH model

The Hamiltonian of the Fermi-Bose-Hubbard model is written usually in the form:

$$H = \frac{U}{2}\sum_i n_i^b(n_i^b - 1) + U'\sum_i n_i^b n_i^f - \mu\sum_i n_i^b - \mu'\sum_i n_i^f + \\ + \sum_{<i,j>} t_{ij} b_i^+ b_j + \sum_{<i,j>} t'_{ij} a_i^+ a_j \tag{2.1}$$

Here U and U' are constants of boson-boson and boson-fermion on-site interactions; μ and μ' are chemical potentials of bosons and fermions, respectively (we consider here the case of repulsive interactions $U > 0, U' > 0$) and t, t' are tunneling amplitudes of bosons (fermions) describing the boson (fermion) hopping between nearest lattice sites.

Let us use, as in [54], the single-site basis of states

$$(n_i^b = n; n_i^f = 0) \equiv |n, i\rangle; \quad (n_i^b = n; n_i^f = 1) \equiv |\widetilde{n}, i\rangle \tag{2.2}$$

where $n_i^b(n_i^f)$ are occupation numbers of bosons (fermions) on the site i, and introduce the Hubbard operators $X_i^{n,m} = |n, i\rangle\langle m, i|$, $\quad X_i^{\widetilde{n},\widetilde{m}} =$

$|\widetilde{n},\rangle\langle\widetilde{m}, i|$, etc. Creating and destroying operators and operators of occupation numbers will express in terms of X-operators in the following way [14, 54].

$$\begin{aligned}
b_i &= \sum_n \sqrt{n+1} X_i^{n,n+1} + \sum_{\widetilde{n}} \sqrt{\widetilde{n}+1} X_i^{\widetilde{n},\widetilde{n}+1} \\
b_i^+ &= \sum_n \sqrt{n+1} X_i^{n+1,n} + \sum_{\widetilde{n}} \sqrt{\widetilde{n}+1} X_i^{\widetilde{n}+1,\widetilde{n}} \\
a_i &= \sum_n X_i^{n,\widetilde{n}} \quad a_i^+ = \sum_n X_i^{\widetilde{n},n} \\
n_i^b &= \sum_n n X^{n,n} + \sum_{\widetilde{n}} \widetilde{n} X^{\widetilde{n},\widetilde{n}}, \quad n_i^f = \sum_{\widetilde{n}} X^{\widetilde{n},\widetilde{n}}
\end{aligned} \tag{2.3}$$

Then, the Hamiltonian in this new representation takes the form:

$$\begin{aligned}
H &= H_0 + H_1^b + H_1^f \qquad (2.4) \\
H_0 &= \sum_{i,n} \lambda_n X_i^{nn} + \sum_{i,\widetilde{n}} \lambda_{\widetilde{n}} X_i^{\widetilde{n}\widetilde{n}} \\
\lambda_n &= \frac{U}{2} n(n-1) - n\mu, \quad \lambda_{\widetilde{n}} = \frac{U}{2}\widetilde{n}(\widetilde{n}-1) - \mu\widetilde{n} - \mu' + U'\widetilde{n} \\
H_1^b &= \sum_{<i,j>} t_{ij} b_i^+ b_j, \quad H_1^f = \sum_{<i,j>} t'_{ij} a_i^+ a_j
\end{aligned}$$

In the case of the hard-core boson approximation ($U \to \infty$) the single-site $|n_i^b, n_i^f\rangle$ basis consists of four states:

$$\begin{aligned}
|0\rangle &= |0, 0\rangle, \qquad |\widetilde{0}\rangle = |0, 1\rangle \\
|1\rangle &= |1, 0\rangle, \qquad |\widetilde{1}\rangle = |1, 1\rangle
\end{aligned} \tag{2.5}$$

In this limit

$$\begin{aligned}
b_i &= X_i^{01} + X^{\widetilde{0}\widetilde{1}}; b_i^+ = X_i^{10} + X^{\widetilde{1}\widetilde{0}} \\
a_i &= X_i^{0\widetilde{0}} + X^{1\widetilde{1}}; a_i^+ = X_i^{\widetilde{0}0} + X^{\widetilde{1}1} \\
n_i^b &= X_i^{11} + X_i^{\widetilde{1}\widetilde{1}}; n_i^f = X_i^{\widetilde{0}\widetilde{0}} + X_i^{\widetilde{1}\widetilde{1}}
\end{aligned} \tag{2.6}$$

$$\lambda_0 = 0; \lambda_1 = -\mu; \lambda_{\widetilde{0}} = -\mu'; \lambda_{\widetilde{1}} = -\mu - \mu' + U' \tag{2.7}$$

and in the expression (2.4) for Hamiltonian of system the restriction $n = 0, 1$ and $\widetilde{n} = \widetilde{0}, \widetilde{1}$ on occupation numbers is imposed. As it was mentioned, we consider the case of the so-called heavy fermions, when the inequalities $t' \ll t, t' \ll U'$ are fulfilled. Our aim consists in study of conditions, at which the MI-SF transition in such a model takes place, in the case when the fermion hopping between lattice sites can be neglected. On this assumption, we will start from Hamiltonian:

$$\hat{H} = \sum_i \left(\lambda_0 X_i^{00} + \lambda_1 X_i^{11} + \lambda_{\widetilde{0}} X_i^{\widetilde{0}\widetilde{0}} + \lambda_{\widetilde{1}} X_i^{\widetilde{1}\widetilde{1}} \right) + \sum_{\langle ij \rangle} t_{ij} b_i^+ b_j \tag{2.8}$$

3. Mean field approximation

Let us introduce the order parameter of BE condensate $\varphi = \langle b_i \rangle = \langle b_i^+ \rangle$. In the case of mean field approximation (MFA):

$$\begin{aligned} & b_i^+ b_j \to \varphi(b_i^+ + b_i) - \varphi^2 \\ & \sum_{ij} t_{ij} b_i^+ b_j = \varphi t_0 \sum_i (b_i^+ + b_i) - N t_0 \varphi^2 \end{aligned} \tag{3.1}$$

(here $t_0 = \sum t_{ij} = -|t_0|, t_0 < 0$)

Then, for initial Hamiltonian after separating the mean field part we will have:

$$H = H_{MF} + \sum_{ij} t_{ij} (b_i^+ - \varphi)(b_i - \varphi) \tag{3.2}$$

Here

$$H_{MF} = \sum_i H_i - N t_0 \varphi^2; \quad H_i = \sum_{pr} H_{pr} X_i^{pr}; \tag{3.3}$$

and

$$||H_{pr}|| = \left(\begin{array}{cccc|c} |0\rangle & |1\rangle & |\widetilde{0}\rangle & |\widetilde{1}\rangle & \\ \hline 0 & t_0\varphi & 0 & 0 & |0\rangle \\ t_0\varphi & -\mu & 0 & 0 & |1\rangle \\ 0 & 0 & -\mu' & t_0\varphi & |\widetilde{0}\rangle \\ 0 & 0 & t_0\varphi & -\mu - \mu' + U' & |\widetilde{1}\rangle \end{array} \right) \tag{3.4}$$

Our next step is the diagonalization:

$$\hat{U}^T * \hat{H} * \hat{U} = \hat{\tilde{H}} \tag{3.5}$$

where : $\hat{U} = \begin{pmatrix} \hat{U}_1 & \hat{0} \\ \hat{0} & \hat{U}_2 \end{pmatrix}$

and:

$\hat{U}_1 = \begin{pmatrix} \cos\psi & -\sin\psi \\ \sin\psi & \cos\psi \end{pmatrix}, \hat{U}_2 = \begin{pmatrix} \cos\widetilde{\psi} & -\sin\widetilde{\psi} \\ \sin\widetilde{\psi} & \cos\widetilde{\psi} \end{pmatrix}$

Here

$$\begin{aligned} \sin 2\psi &= \frac{t_0\varphi}{\sqrt{\mu^2/4 + t_0^2\varphi^2}}, \\ \sin 2\widetilde{\psi} &= \frac{t_0\varphi}{\sqrt{(U' - \mu)^2/4 + t_0^2\varphi^2}} \end{aligned} \tag{3.6}$$

Then we will get the diagonal single-site part (which is as well a mean-field one) of Hamiltonian:

$$\hat{H}_i = \sum_{p'} \varepsilon_{p'} X_i^{p'p'} - N t_0 \varphi^2, \tag{3.7}$$

where $p' = 0', 1', \widetilde{0}', \widetilde{1}'$ are indices, which denote the states of new basis,

$$\begin{aligned} \varepsilon_{0',1'} &= -\frac{\mu}{2} \pm \sqrt{\frac{\mu^2}{4} + t_0^2\varphi^2}, \\ \varepsilon_{\widetilde{0}',\widetilde{1}'} &= -\mu' - \frac{\mu}{2} + \frac{U'}{2} \pm \sqrt{\frac{(U' - \mu)^2}{4} + t_0^2\varphi^2} \end{aligned} \tag{3.8}$$

For Bose-operators we will have in new basis:

$$\begin{aligned} b_i = & \frac{1}{2}\sin(2\psi)(X_i^{0'0'} - X_i^{1'1'}) + \frac{1}{2}\sin(2\widetilde{\psi})(X_i^{\widetilde{0}'\widetilde{0}'} - X_i^{\widetilde{1}'\widetilde{1}'}) + \\ & + \cos^2\psi X_i^{0'1'} - \sin^2\psi X_i^{1'0'} + \cos^2\widetilde{\psi} X_i^{\widetilde{0}'\widetilde{1}'} - \sin^2\widetilde{\psi} X_i^{\widetilde{1}'\widetilde{0}'} \end{aligned}$$

4. Thermodynamic potential in the mean field approximation

The partition function in MFA is equal to:

$$\begin{aligned} Z_{MF} &= Sp e^{-\beta H_{MF}} = e^{\beta N t_0 \varphi^2} \prod_i Sp e^{-\beta \sum\limits_{pr} H_{pr} X_i^{pr}} = \\ &= e^{\beta N t_0 \varphi^2} \prod_i e^{-\beta \sum\limits_{p'} \varepsilon_{p'} X_i^{p'p'}} = e^{\beta N t_0 \varphi^2} Z_0^N \end{aligned} \tag{4.1}$$

where

$$Z_0 = e^{-\beta\varepsilon_{0'}} + e^{-\beta\varepsilon_{1'}} + e^{-\beta\varepsilon_{\widetilde{0'}}} + e^{-\beta\varepsilon_{\widetilde{1'}}} \tag{4.2}$$

The grand canonical potential is:

$$\Omega_{MF} = -\theta \ln Z_{MF} = N|t_0|\varphi^2 - N\Theta \ln Z_0 \tag{4.3}$$

or

$$\Omega_{MF}/N = |t_0|\varphi^2 - \theta \ln Z_0 \tag{4.4}$$

(here we take into account that $t_0 = -|t_0|$). The equilibrium value of the order parameter φ can be found from the global minimum condition of Ω.

We have an equation

$$\frac{\partial(\Omega_{MF}/N)}{\partial\varphi} = 2|t_0|\varphi - \frac{\theta}{Z_0}\frac{\partial Z_0}{\partial\varphi} = 0 \tag{4.5}$$

or

$$2|t_0|\varphi + \sum_{p'}\langle X^{p'p'}\rangle \frac{\partial\varepsilon_{p'}}{\partial\varphi} = 0 \tag{4.6}$$

Here:

$$\langle X^{p'p'}\rangle = \frac{1}{Z_0}e^{-\beta\varepsilon_{p'}} \tag{4.7}$$

Using that:

$$\begin{aligned}\frac{\partial\varepsilon_{0',1'}}{\partial\varphi} &= \pm t_0 \sin 2\psi = \mp|t_0|\sin 2\psi \\ \frac{\partial\varepsilon_{\widetilde{0'},\widetilde{1'}}}{\partial\varphi} &= \pm t_0 \sin 2\widetilde{\psi} = \mp|t_0|\sin 2\widetilde{\psi},\end{aligned} \tag{4.8}$$

we will get from (4.6)

$$\varphi = \frac{1}{2}\sin 2\psi\left(\langle X^{0'0'}\rangle - \langle X^{1'1'}\rangle\right) + \frac{1}{2}\sin 2\widetilde{\psi}\left(\langle X^{\widetilde{0'}\widetilde{0'}}\rangle - \langle X^{\widetilde{1'}\widetilde{1'}}\rangle\right) \tag{4.9}$$

or in the explicit form,

$$\varphi = \frac{|t_0|\varphi}{2}\left[\frac{\langle X^{1'1'}\rangle - \langle X^{0'0'}\rangle}{\sqrt{\frac{\mu^2}{4} + t_0^2\varphi^2}} + \frac{\langle X^{\widetilde{1'}\widetilde{1'}}\rangle - \langle X^{\widetilde{0'}\widetilde{0'}}\rangle}{\sqrt{\frac{(U'-\mu)^2}{4} + t_0^2\varphi^2}}\right] \tag{4.10}$$

This equation has trivial $\varphi = 0$ and non-trivial $\varphi \neq 0$ solutions, the second can be obtained from the equation:

$$\frac{1}{|t_0|} = \frac{\langle X^{1'1'}\rangle - \langle X^{0'0'}\rangle}{2\sqrt{\frac{\mu^2}{4} + t_0^2\varphi^2}} + \frac{\langle X^{\widetilde{1'}\widetilde{1'}}\rangle - \langle X^{\widetilde{0'}\widetilde{0'}}\rangle}{2\sqrt{\frac{(U'-\mu)^2}{4} + t_0^2\varphi^2}} \tag{4.11}$$

When we have several solutions in this equation – we will consider only that, which are related to minimum of Ω_{MF}

5. Averages $\langle b_i\rangle$, $\langle b_i^+\rangle$ and equation for φ

Let's us to apply the unitary transformation $\hat{U}^T(...)\hat{U}$ to operators X_i^{01} and $X_i^{\widetilde{0}\widetilde{1}}$; which, in the matrix form, are:

$$||X_i^{01}|| = \begin{pmatrix} 0 & 1 & 0 & 0 \\ 0 & 0 & 0 & 0 \\ 0 & 0 & 0 & 0 \\ 0 & 0 & 0 & 0 \end{pmatrix}, \quad ||X_i^{\widetilde{0}\widetilde{1}}|| = \begin{pmatrix} 0 & 0 & 0 & 0 \\ 0 & 0 & 0 & 0 \\ 0 & 0 & 0 & 1 \\ 0 & 0 & 0 & 0 \end{pmatrix} \tag{5.1}$$

We will get:

$$||\hat{U}^T X_i^{01}\hat{U}|| = \begin{pmatrix} \sin\psi\cos\psi & \cos^2\psi & 0 & 0 \\ -\sin^2\psi & -\sin\psi\cos\psi & 0 & 0 \\ 0 & 0 & 0 & 0 \\ 0 & 0 & 0 & 0 \end{pmatrix} \tag{5.2}$$

and

$$||\hat{U}^T X_i^{\widetilde{0}\widetilde{1}}\hat{U}|| = \begin{pmatrix} 0 & 0 & 0 & 0 \\ 0 & 0 & 0 & 0 \\ 0 & 0 & \sin\widetilde{\psi}\cos\widetilde{\psi} & \cos^2\widetilde{\psi} \\ 0 & 0 & -\sin^2\widetilde{\psi} & -\sin\widetilde{\psi}\cos\widetilde{\psi} \end{pmatrix} \tag{5.3}$$

In the transformed basis representation:

$$\begin{aligned}\hat{U}^T X_i^{01}\hat{U} &= \cos^2\psi X_i^{0'1'} + \sin\psi\cos\psi(X_i^{0'0'} - X_i^{1'1'}) - \sin^2\psi X_i^{1'0'} \\ \hat{U}^T X_i^{\widetilde{0}\widetilde{1}}\hat{U} &= \cos^2\widetilde{\psi} X^{\widetilde{0'}\widetilde{1'}} + \sin\widetilde{\psi}\cos\widetilde{\psi}(X^{\widetilde{0'}\widetilde{0'}} - X^{\widetilde{1'}\widetilde{1'}}) - \sin^2\widetilde{\psi} X^{\widetilde{1'}\widetilde{0'}}\end{aligned} \tag{5.4}$$

After averaging with the aid of H_{MF} Hamiltonian:

$$\langle X_i^{01}\rangle = \frac{1}{Z_0}Sp(X_i^{01}e^{-\beta H_{MF}}) = \frac{1}{Z_0}Sp(\hat{U}^T X_i^{01}\hat{U}e^{-\beta H_{MF}}) \tag{5.5}$$

On the new basis the Hamiltonian H_{MF} is diagonal; because of that, the averages of diagonal operators $X_i^{p'p'}$ $(p' = 0', 1', \widetilde{0}', \widetilde{1}')$ only will be non-zero. Thus

$$\langle X_i^{01} \rangle = \frac{1}{2} \sin 2\psi \left(\langle X^{0'0'} \rangle - \langle X^{1'1'} \rangle \right) \tag{5.6}$$
$$\langle X_i^{\widetilde{0}\widetilde{1}} \rangle = \frac{1}{2} \sin 2\widetilde{\psi} \left(\langle X^{\widetilde{0}'\widetilde{0}'} \rangle - \langle X^{\widetilde{1}'\widetilde{1}'} \rangle \right)$$

As a result, we have:

$$\varphi = \langle b_i \rangle = \langle X_i^{01} \rangle + \langle X_i^{\widetilde{0}\widetilde{1}} \rangle = \frac{1}{2} \sin 2\psi \left(\langle X^{0'0'} \rangle - \langle X^{1'1'} \rangle \right) + $$
$$+ \frac{1}{2} \sin 2\widetilde{\psi} \left(\langle X^{\widetilde{0}'\widetilde{0}'} \rangle - \langle X^{\widetilde{1}'\widetilde{1}'} \rangle \right) \tag{5.7}$$

So, we came to the same equation for φ as we have got from the extremum condition for grand canonical potential.

6. The spinodal equation

If in the equation (4.11) we substitute $\varphi = 0$, we will have the condition for second order phase transition to SF phase (if this transition is possible). In general, it is the condition of instability of normal (MI) phase with respect to the Bose-Einstein condensate appearance (in figures it corresponds to spinodal lines).

The equation (4.11) can be rewritten as:

$$\frac{1}{|t_0|} = \frac{\langle X^{1'1'} \rangle - \langle X^{0'0'} \rangle}{\varepsilon_{0'} - \varepsilon_{1'}} + \frac{\langle X^{\widetilde{1}'\widetilde{1}'} \rangle - \langle X^{\widetilde{0}'\widetilde{0}'} \rangle}{\varepsilon_{\widetilde{0}'} - \varepsilon_{\widetilde{1}'}} \tag{6.1}$$

If $\varphi \to 0$,

$$\varepsilon_{0'} = \begin{cases} \lambda_0, \mu > 0 \\ \lambda_1, \mu < 0 \end{cases} ; \quad \varepsilon_{\widetilde{0}} = \begin{cases} \lambda_{\widetilde{1}}, \mu < U' \\ \lambda_{\widetilde{0}}, \mu > U' \end{cases} \tag{6.2}$$
$$\varepsilon_{1'} = \begin{cases} \lambda_1, \mu > 0 \\ \lambda_0, \mu < 0 \end{cases} ; \quad \varepsilon_{\widetilde{1}} = \begin{cases} \lambda_{\widetilde{0}}, \mu < U' \\ \lambda_{\widetilde{1}}, \mu > U' \end{cases}$$

It is seen that we can divide the μ axis on three regions (1) $\mu < 0$; (2) $0 < \mu < U'$; (3) $\mu > U'$ (when $U' > 0$). For all these regions the equation (6.1) takes the form:

$$\frac{1}{|t_0|} = \frac{\langle X^{00} \rangle - \langle X^{11} \rangle}{\lambda_1 - \lambda_0} + \frac{\langle X^{\widetilde{0}\widetilde{0}} \rangle - \langle X^{\widetilde{1}\widetilde{1}} \rangle}{\lambda_{\widetilde{1}} - \lambda_{\widetilde{0}}} \tag{6.3}$$

It can be rewritten as:

$$\frac{1}{|t_0|} = \frac{\langle X^{11} \rangle - \langle X^{00} \rangle}{\mu} + \frac{\langle X^{\widetilde{0}\widetilde{0}} \rangle - \langle X^{\widetilde{1}\widetilde{1}} \rangle}{U' - \mu} \tag{6.4}$$

The equation (6.3) is the same as obtained in [51] from the condition of divergence of the bosonic Green's function (calculated in the random phase approximation) at $\omega = 0, \mathbf{q} = \mathbf{0}$. In this way it is the condition of instability of the phase with $\varphi = 0$. Therefore, the equation (6.3) is an equation for spinodal line.

7. Spinodals at $T = 0$

When $T = 0$, averages $\langle X^{p'p'} \rangle, \langle X^{\widetilde{p}'\widetilde{p}'} \rangle$ are different from zero only for lowest energy level. Here the three cases can be separated out.

1) $\mu' < 0$

Here, at $\mu < 0$ the ground state is the state is $|0\rangle$, and at $\mu > 0$ the ground state is $|1\rangle$. Respectively, in the first one from these cases $\langle X^{00} \rangle = 1$, while in the second one $\langle X^{11} \rangle = 1$ (other averages are equal to zero). The equation (6.4) can be written now as:

$$\frac{1}{|t_0|} = \begin{cases} -\frac{1}{\mu}, & \mu < 0 \\ \frac{1}{\mu}, & \mu > 0 \end{cases} \tag{7.1}$$

It follows from here that

$$\mu = \begin{cases} t_0, & \mu > 0 \\ -t_0, & \mu < 0 \end{cases} \tag{7.2}$$

This is the spinodal equation for $\mu' < 0$.

2) $\mu' > U'$

The change of ground state takes place when $\mu = U'$. For $\mu < U'$ the state $|\widetilde{0}\rangle$ is the ground one, and for $\mu > U'$ it is the state $|\widetilde{1}\rangle$. Respectively, at $\mu < U', \langle X^{\widetilde{0}\widetilde{0}} \rangle = 1$ and at $\mu > U', \langle X^{\widetilde{1}\widetilde{1}} \rangle = 1$. The equation (6.4) takes now the form:

$$\frac{1}{|t_0|} = \begin{cases} \frac{1}{U' - \mu}, & \mu < U' \\ \frac{1}{\mu - U'}, & \mu > U' \end{cases} \tag{7.3}$$

In this case the following lines will be the lines of spinodal:

$$\begin{cases} \mu = U' + t_0, \mu > U' \\ \mu = U' - t_0, \mu < U' \end{cases} \tag{7.4}$$

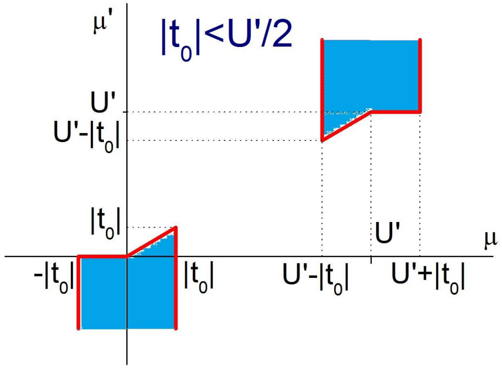

Fig.1a Instability region of MI phase (at $T=0$); the case $|t_0|<U'/2$

3) $0<\mu'<U'$

The change of ground state takes place now when $\mu=\mu'$. For $\mu<\mu'$ t such a state is $|\tilde{0}\rangle$, and for $\mu>\mu'$ it is the state $|1\rangle$. Respectively, at $\mu<\mu', \langle X^{\widetilde{00}}\rangle=1$ and for $\mu>\mu', \langle X^{11}\rangle=1$. For spinodal we will have now the equation:

$$\frac{1}{|t_0|}=\frac{\langle X^{11}\rangle}{\mu}+\frac{\langle X^{\widetilde{00}}\rangle}{U'-\mu} \tag{7.5}$$

It follows from here that, $\mu=U'-|t_0|$ when $\mu<\mu'$, and $\mu=|t_0|$ when $\mu>\mu'$. In the case $|t_0|<U'$, the solution $\mu=\mu'$ also appears. When $\mu'>U'/2$, it exists for $U'-\mu'<|t_0|<\mu'$, and at $\mu'<U'/2$ it exists for $\mu'<|t_0|<U'-\mu'$. If $|t_0|\geq U'$, the solution $\mu=\mu'$ disappears.

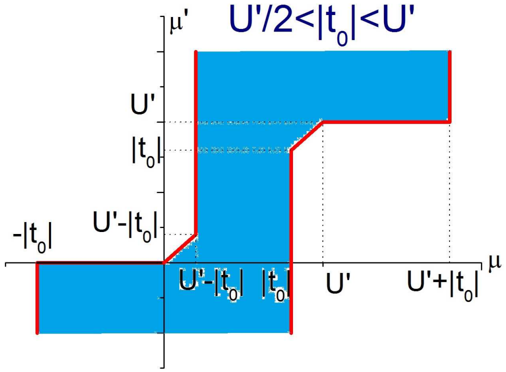

Fig.1b Instability region of MI phase (at $T=0$); the case $\frac{U'}{2}<|t_0|<U'$

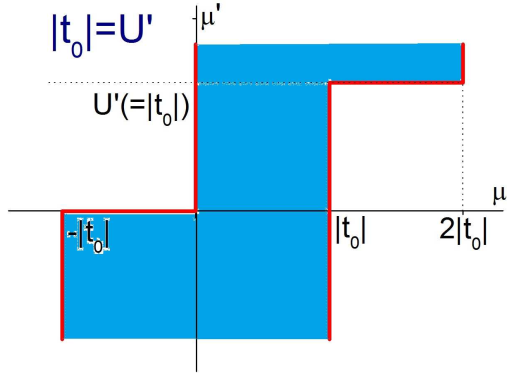

Fig.1c Instability region of MI phase (at $T=0$); the case $|t_0|=U'$

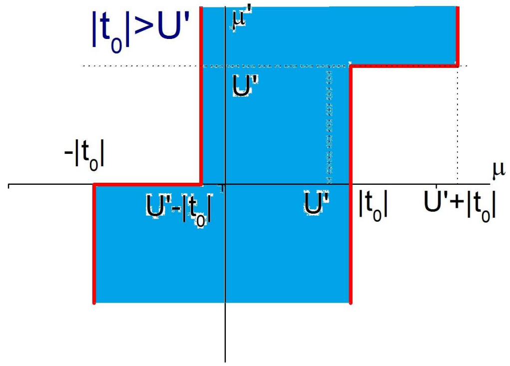

Fig.1d Instability region of MI phase (at $T=0$); the case $|t_0|>U'$

The lines of spinodales are broken and much differ for cases $|t_0|\geq U', U'>|t_0|>U'/2, |t_0|<U'/2$. As a result, the areas of absolute instability of the normal phase (calculated at $T=0$) possess the different shapes. These areas are shown in figures 1a–1d.

8. $\varphi(\mu)$ and $\Omega(\mu)$ dependences at $T=0$

One can find the dependences of order parameter φ and grand canonical potential Ω upon the chemical potential of bosons at different values of temperature and μ' using the equation (4.11).

In the limit $T\to 0$ only averages related to the ground state contribute to the right-hand side of the equation. With the change of φ the ground state can be reconstructed and this makes the problem of determination of solutions for order parameter self-consistent. This problem can have analytical solution, when states with fermion and without fermion are not mutually mixed. This can be achieved when μ' takes values which are far-off the $[0, U']$ interval.

When we have the large in modulus and negative μ' values, the state $|1'\rangle$ is the ground one and the equation (4.11) reduces in this case:

$$\frac{1}{|t_0|} = \frac{1}{2\sqrt{\frac{\mu^2}{4} + t_0^2\varphi^2}} \tag{8.1}$$

Then:

$$\varphi = \frac{1}{2}\sqrt{1 - \mu^2/t_0^2} \tag{8.2}$$

In a positive region, when $\mu' \gg U'$, the state $|\widetilde{1'}\rangle$ is the ground one; respectively, we have an equation:

$$\frac{1}{|t_0|} = \frac{1}{2\sqrt{\frac{(U'-\mu)^2}{4} + t_0^2\varphi^2}} \tag{8.3}$$

In this case:

$$\varphi = \frac{1}{2}\sqrt{1 - (\mu - U')^2/t_0^2} \tag{8.4}$$

The dependences of functions (8.2) and (8.4) on μ are presented in figures 2a, 2b.

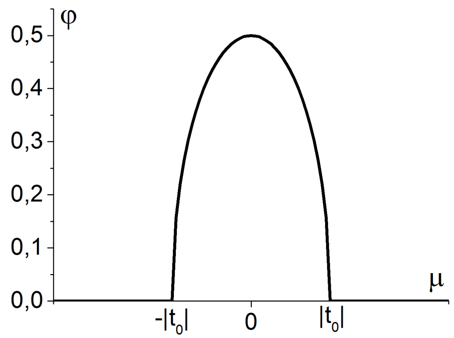

Fig.2a Order parameter as function of μ for $\mu' < 0, |\mu'| \ll U'$

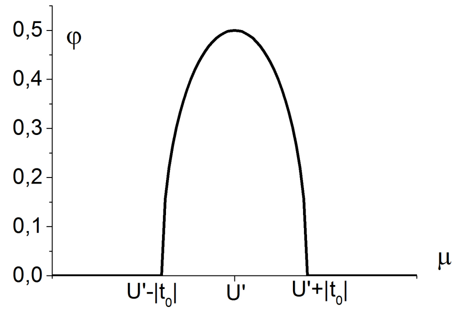

Fig.2b Order parameter as function of μ for $\mu' \gg U'$

In the region of intermediate values of μ' (especially at $0 \leq \mu' \leq U'$), the mixing of “tilded” and “untilded” states leads to deformation of the curve $\varphi(\mu)$. In the figures 3a, 3b, 3c one can see the plots of order parameter φ as function of chemical potential of bosons μ for different values of chemical potential of fermions μ'. These curves are obtained numerically from the equation (4.11) in the case $T = 0$.

One can see that in the vicinity of $\mu' = 0$ and $\mu' = U'$ values the $\varphi(\mu)$ dependence has a reverse course and S-like behaviour. This is an evidence of possibility of the first order phase transition (instead of the

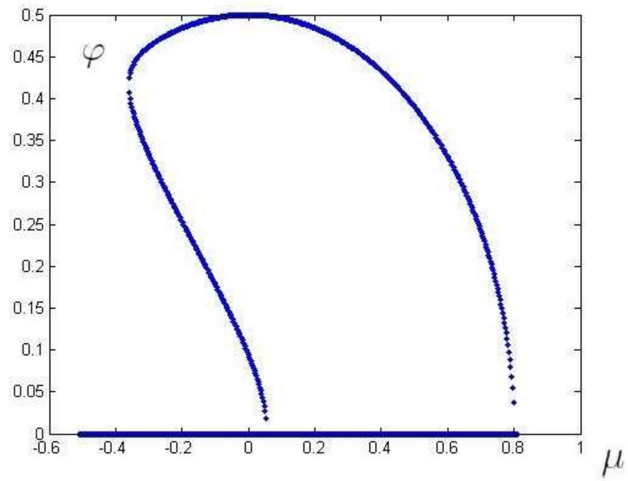

Fig.3a Order parameter φ as function of μ for $T \to 0; \mu' = 0.1, U' = 1, |t_0| = 0.8$

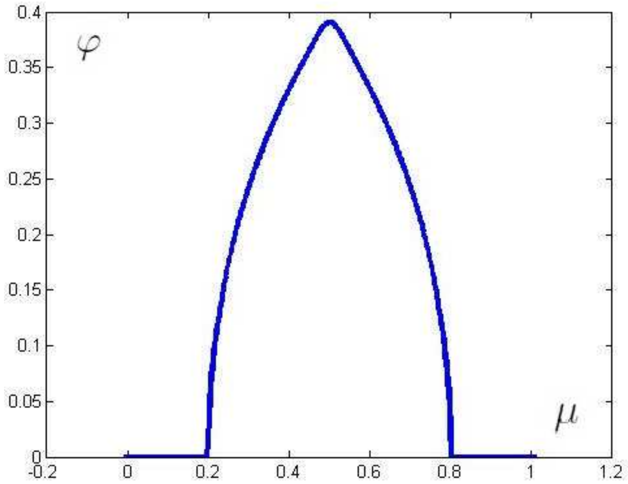

Fig.3b Order parameter φ as function of μ for $T \to 0; \mu' = 0.5, U' = 1, |t_0| = 0.8$

second order one). This conclusion can be confirmed by calculation of grand canonical potential $\Omega_{MF}(\mu)$ as function of μ.

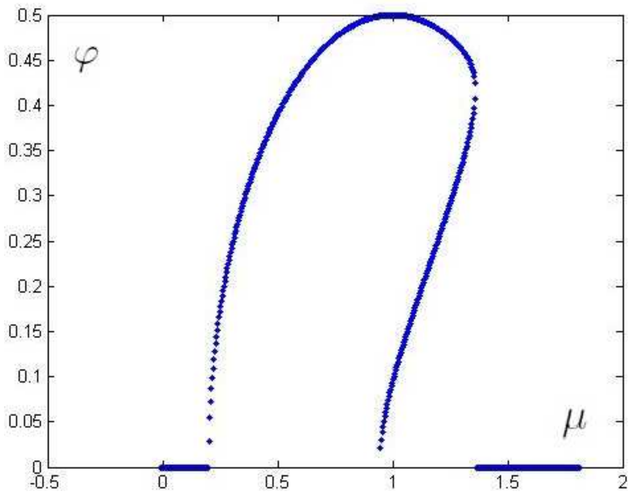

Fig.3c Order parameter φ as function of μ for $T \to 0; \mu' = 0.9, U' = 1, |t_0| = 0.8$

In the case of large negative values of chemical potential μ', when at $T = 0$ only state $|1'\rangle$ remains:

$$\Omega_{MF}/N \to |t_0|\varphi^2 - \theta \ln e^{-\beta\varepsilon_{1'}} = |t_0|\varphi^2 - \frac{\mu}{2} - \sqrt{\frac{\mu^2}{4} + t_0^2\varphi^2} \qquad (8.5)$$

Using expression (8.2) we have:

$$\Omega_{MF}/N = -\frac{(\mu^2 + |t_0|^2)}{4|t_0|} \qquad (8.6)$$

At the same time, at $\varphi = 0$ the ground state in the region $\mu' < 0$ is the state $|0\rangle$ for $\mu < 0$ and the state $|1\rangle$ for $\mu > 0$. Then:

$$\Omega_{MF}/N|_{\varphi=0} = \begin{cases} 0, & \mu < 0 \\ -\mu, & \mu > 0 \end{cases} \qquad (8.7)$$

Plots of functions (8.6) and (8.7) are presented in the figure 4a.

One can see that derivatives $\frac{\partial\Omega_{MF}}{\partial\mu}$ and $\frac{\partial\Omega_{MF}|_{\varphi=0}}{\partial\mu}$ coincide in the points $\mu = \pm|t_0|$ that limit the interval of μ values with $\varphi \neq 0$. This verifies the second order of the phase transition to the phase with BE condensate here.

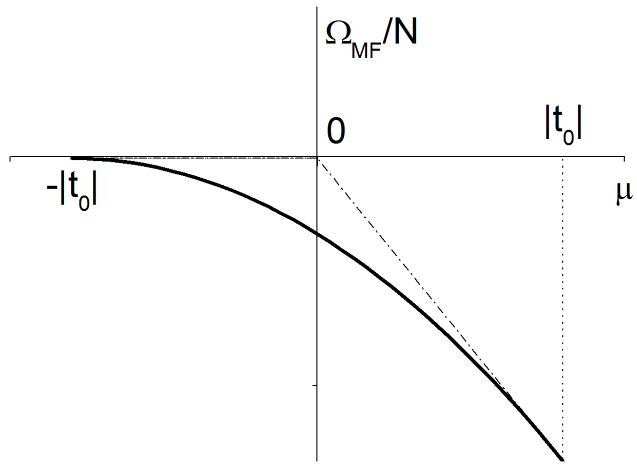

Fig.4a Grand canonical potentials Ω_{MF}/N (solid line) and $(\Omega_{MF}/N)_{\varphi=0}$ (dotted line) as functions of μ at $\mu' < 0, |\mu'| \ll U', |t_0| = 0.8$ $(T \to 0)$

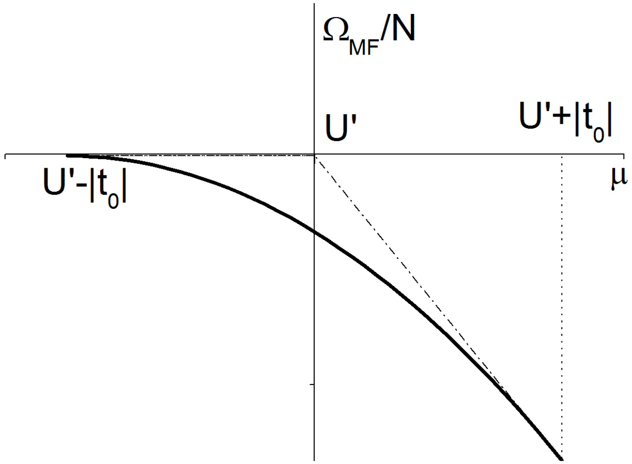

Fig.4b Grand canonical potentials Ω_{MF}/N (solid line) and $(\Omega_{MF}/N)_{\varphi=0}$ (dashed line) as functions of μ at $\mu' > 0, \mu' \gg U', |t_0| = 0.8$ $(T \to 0)$

The function $\Omega_{MF}/N(\mu)$ has the similar character in other limiting case, namely the case of large positive values of μ'. Here:

$$\Omega_{MF}/N = -\frac{((\mu - U')^2 + |t_0|^2)}{4|t_0|} - \mu'$$
$$\Omega_{MF}/N|_{\varphi=0} = \begin{cases} -\mu', \mu < U' \\ U' - \mu - \mu', \mu > U' \end{cases} \tag{8.8}$$

(see the figure 4b). Here the second order phase transition also takes place.

The result of numerical calculations of function $\Omega_{MF}/N(\mu)$ in the case of intermediate values of μ' (done with the help of calculated earlier $\varphi(\mu)$ dependences) are shown in figures 5a, 5b, 5c. Here and hereafter numerical values of parameters are given in the U' units.

In the cases when the function $\varphi(\mu)$ has a reverse course, one can see the so-called "fishtails" in the behaviour of the grand canonical potential where the intersection points of lowest curves correspond to the first order phase transitions (phase transitions on the other side of the interval of non-zero φ values are of the second order). Values of μ at which there the first order phase transitions exist, are shifted relatively the spinodal line points (near $\mu' = 0$ to the left and near $\mu' = U'$ to the right). As a

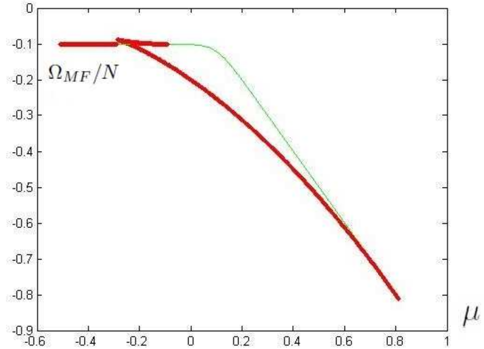

Fig.5a Grand canonical potential as function of μ at $T \to 0, \mu' = 0.1, |t_0| = 0.8$

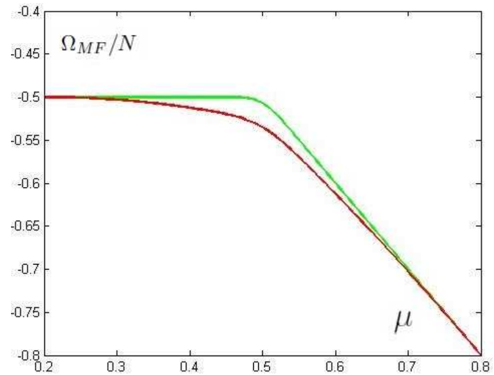

Fig.5b Grand canonical as function of μ at $T \to 0, \mu' = 0.5$

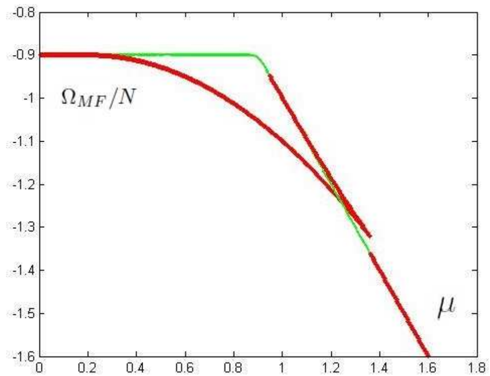

Fig.5c Grand canonical potential as function of μ at $T \to 0, \mu' = 0.9$

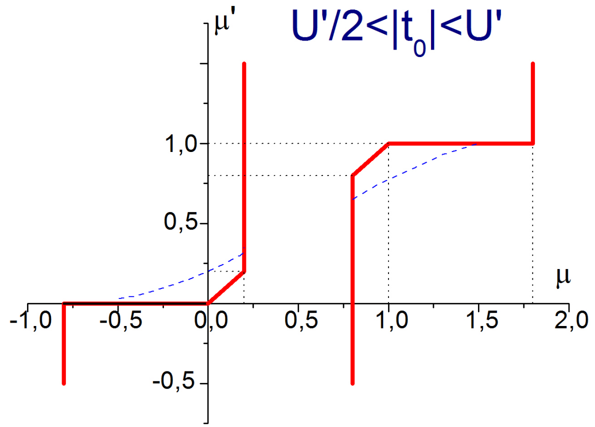

Fig.6 Limits of the SF phase area (including the 1st(2nd) order phase transition lines shown by dotted (solid) curves), $T \to 0$, $t_0 = 0.8U'$

result – the region of existence of SF phase at $T = 0$ is wider then the limited by spinodals.

Described effect of the phase transition order change disappears when chemical potential μ' is placed near middle of the $[0, U']$ interval (see figure 6). The point $\mu' = U'/2$ is a special one. With decreasing of μ', the fragmentation of SF region on two parts takes place at this point.

9. Phase transitions at $T \neq 0$

The investigation similar to the previous one can be done in the case of non-zero temperature. Lets first take a look on spinodals – the curves, that determine the borders of the normal phase stability region. When $T \neq 0$, they are described by the equation (6.4). The solutions of this equation on the plane (T, μ) for different values of μ' are shown in figures 7a–7d and 8a–8d.

Outside the $[0, U']$ interval for μ', the curves of spinodals have the usual dome-like shape. Attaining to this area, the curves undergo an appreciable deformation, and when they enter inside, the regions with two temperatures of instability corresponding to one value of μ appear. With the change of T the "re-entrant" transitions became possible. But, to get the real (T, μ) phase diagrams one need to investigate the grand canonical potential behaviour in such regions.

In the figures 3a, 5a, 9a,b, 10a,b one can see how the shape of curves for $\varphi(\mu)$ and Ω_{MF}/N changes with the increase of temperature in the

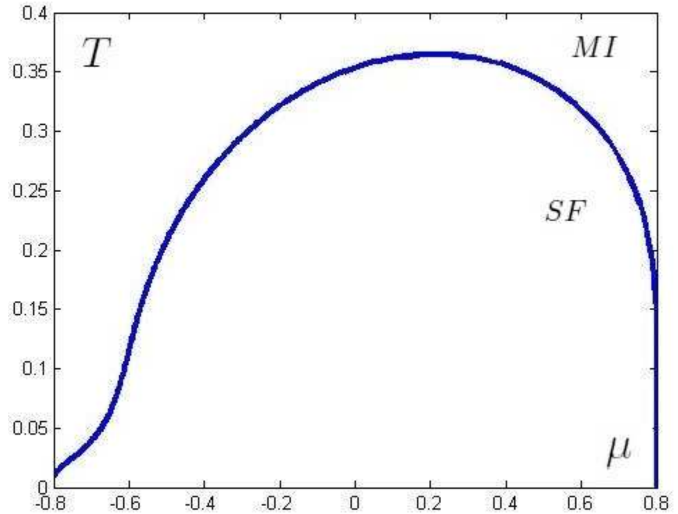

Fig.7a (T, μ) phase diagram; $|t_0| = 0.8, U' = 1, \mu' = -0.05$

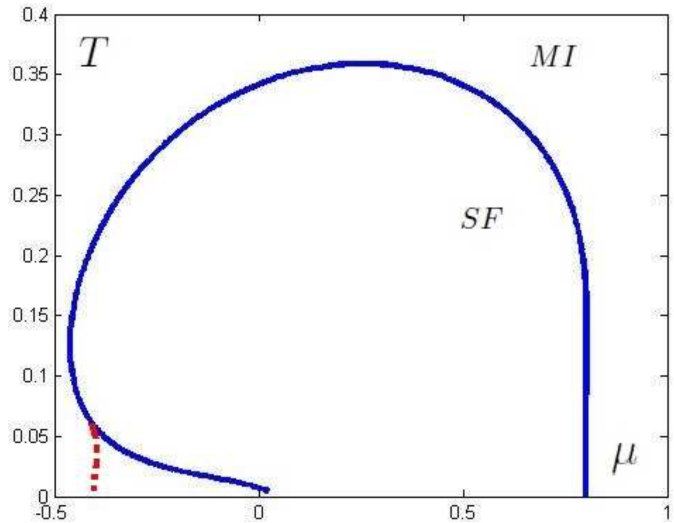

Fig.7b (T, μ) phase diagram; $|t_0| = 0.8, U' = 1, \mu' = 0.05$

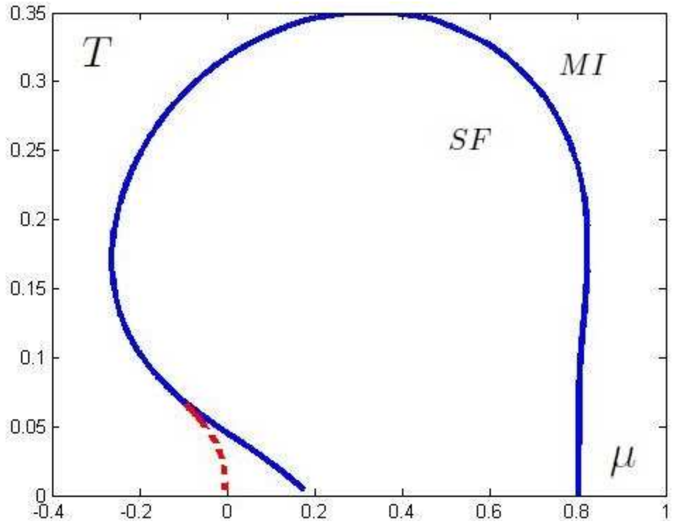

Fig.7c (T, μ) phase diagram; $|t_0| = 0.8, U' = 1, \mu' = 0.2$

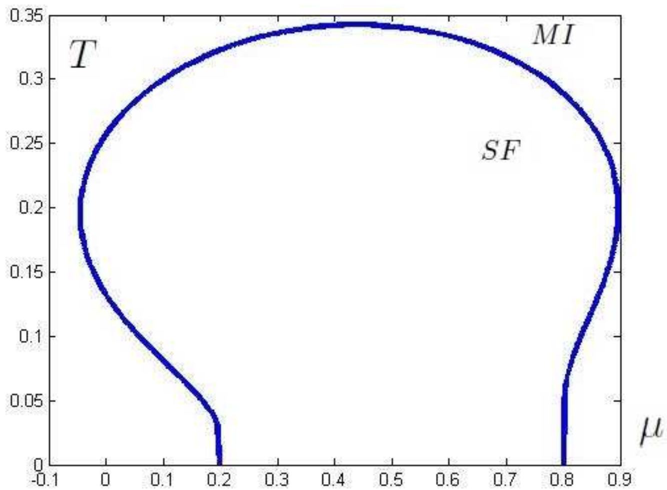

Fig.7d (T, μ) phase diagram; $|t_0| = 0.8, U' = 1, \mu' = 0.4$

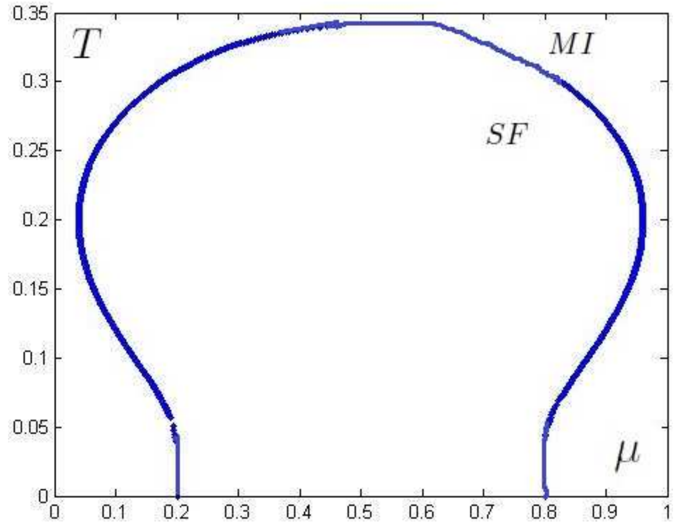

Fig.8a (T, μ) phase diagram; $|t_0| = 0.8, U' = 1, \mu' = 0.5$

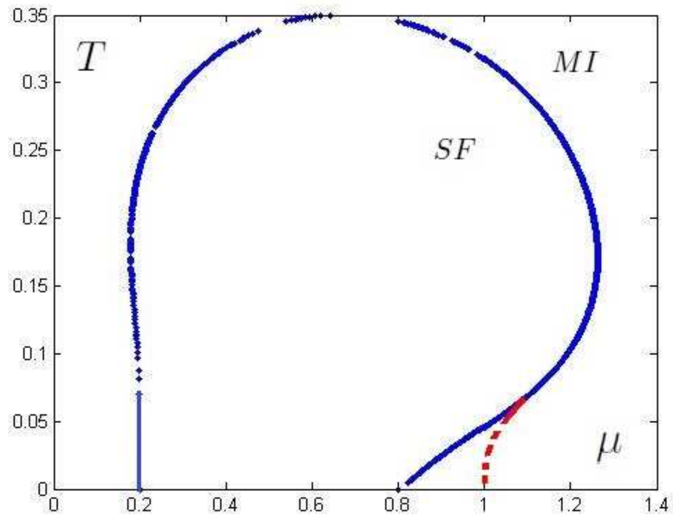

Fig.8b (T, μ) phase diagram; $|t_0| = 0.8, U' = 1, \mu' = 0.8$

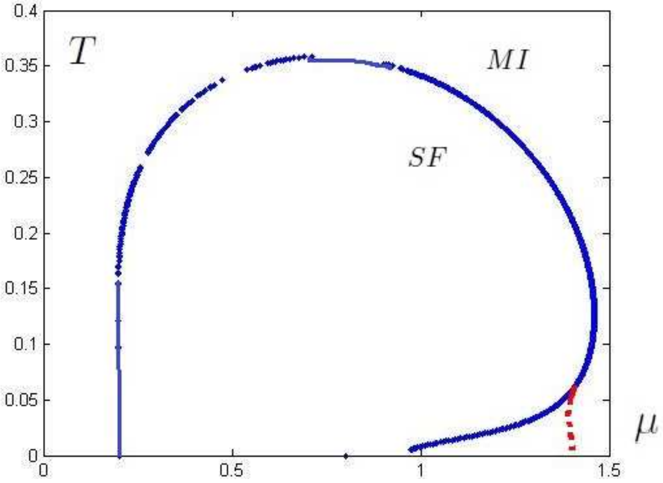

Fig.8c (T, μ) phase diagram; $|t_0| = 0.8, U' = 1, \mu' = 0.95$

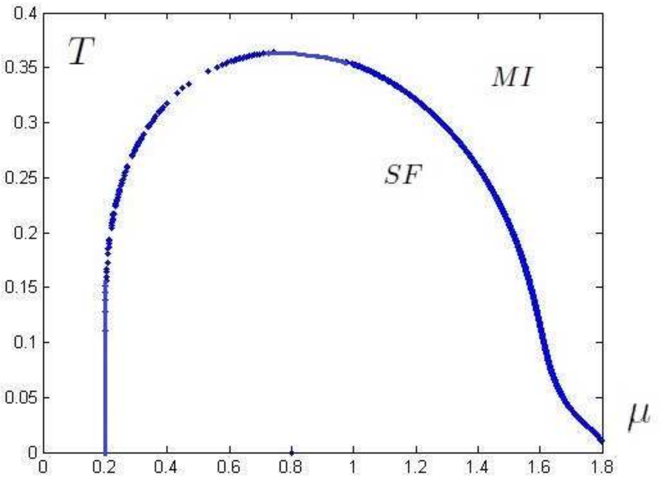

Fig.8d (T, μ) phase diagram; $|t_0| = 0.8, U' = 1, \mu' = 1.05$

region of parameters values, where at $T = 0$ we have the first order phase transition. At higher temperatures the reverse course of $\varphi(\mu)$ function and "fishtail" of Ω_{MF}/N gradually decrease and disappear. At some temperature, that corresponds to tricritical point, the order of phase transition changes from first to second. At the further increase of temperature the curves of phase transitions coincide with the spinodal lines. It is shown in figures 7b,c and 8b,c where dotted lines are the lines of the first order phase transitions. They are present in the phase diagrams in the cases when $0 < \mu' \lesssim 0.3U'$ ans $0.7U' \lesssim \mu < U'$. From figures one can see that in almost all cases for $0 < \mu' < U'$ interval there are regions where "re-entrant" transitions take place. In these cases the SF phase exists as intermediate one between temperature regions where the normal phase is stable.

It is worthy to consider, besides previously analyzed, the phase diagrams (μ', μ) at nonzero temperatures. In the region of temperatures above the tricritical ones (which reach a maximum of the order of $0,075U'$, as it seen from figures 7b,7c,8b,8c) the phase transition lines coincide with spinodales; the transitions, as such, are of the 2nd order. Borders between phases are determined in this case by the equation (5.4) where

$$\langle X^{nn} \rangle = Z_0^{-1} \mid_{\varphi=0} e^{-\beta\lambda_n}; \quad \langle X^{\tilde{n}\tilde{n}} \rangle = Z_0^{-1} \mid_{\varphi=0} e^{-\beta\lambda_{\tilde{n}}} \tag{9.1}$$

$$Z_0 \mid_{\varphi=0} = \sum_{n=0}^{1} e^{-\beta\lambda_n} + \sum_{n=\tilde{0}}^{\tilde{1}} e^{-\beta\lambda_{\tilde{n}}}$$

and λ_n and $\lambda_{\tilde{n}}$ are specified in (1.5).

In the case $U'/2 < |t_0| < U'$, the obtained numerically (μ', μ) phase diagrams are presented in figure 6. The change of shape of the SF phase region during gradual raisins of temperature, starting form $\theta = 0,1U'$, is shown. This region is simply connected at $T = 0$. However, as is seen from μ' versus μ plots, at certain (critical) temperature θ_c the change of topology of phase diagrams takes place. The SF phase region becomes biconnected (it occurs at $\theta_c \cong 0,341U'$ when $|t_0| = 0,8U'$). Such a splitting into two parts is realized at point with coordinates $\mu = \mu' = 0,5U'$. For these values of chemical potentials we have at $T = \theta_c$ the second order phase transition from the SF to MI phase.

At the further increase of temperature the separated SF phase regions move away one from another and become narrower. Finally, they disappear at $T_c^0 = |t_0|/2$. This temperature is obtained from the equations

$$\frac{1}{|t_0|} = \frac{1}{\mu} \tanh \frac{\beta\mu}{2} \tag{9.2}$$

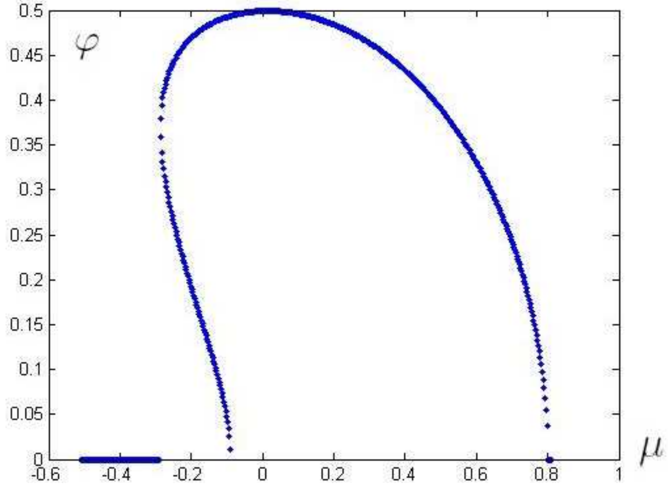

Fig.9a Order parameter φ as function of μ;
$T = 0.03, \mu' = 0.1, |t_0| = 0.8$, U'=1

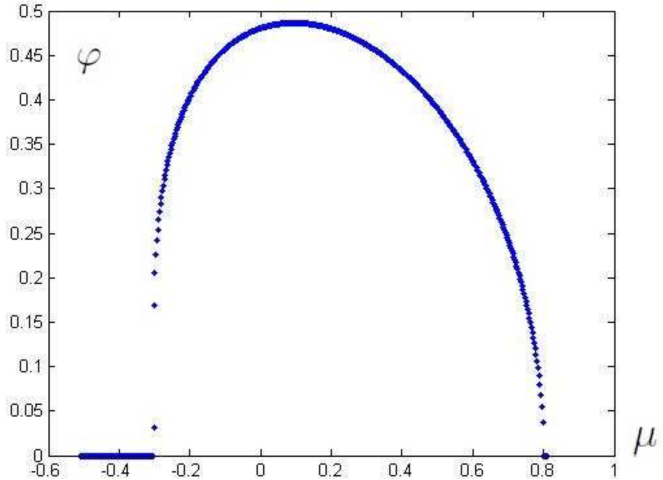

Fig.9b Order parameter φ as function of μ;
$T = 0.07, \mu' = 0.1, |t_0| = 0.8, U' = 1$

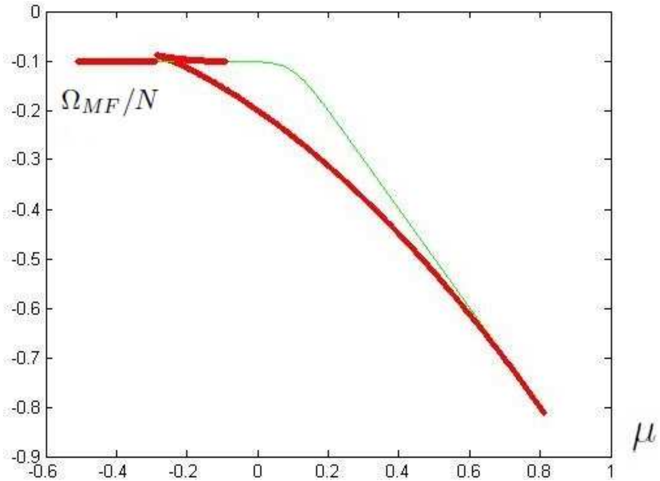

Fig.10a Grand canonical potential as function of μ at
$T = 0.03, \mu' = 0.1, |t_0| = 0.8, U' = 1$

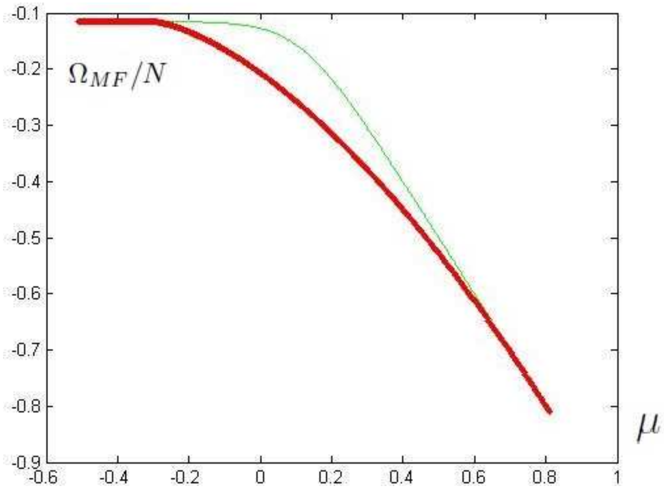

Fig.10b Grand canonical potential as function of μ at
$T = 0.07, \mu' = 0.1, |t_0| = 0.8, U' = 1$

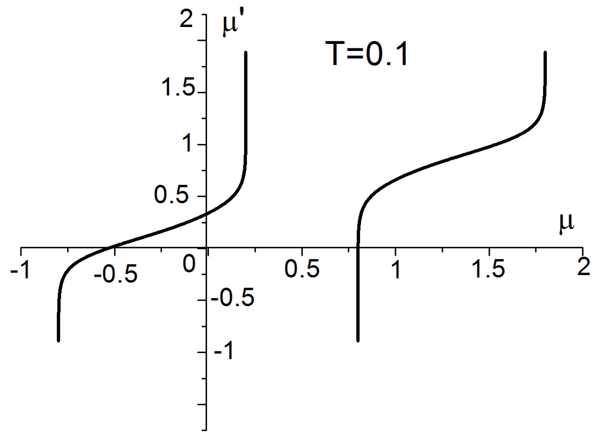

Fig.11a (μ, μ') phase diagram at $T = 0.1, |t_0| = 0.8, U' = 1$

or

$$\frac{1}{|t_0|} = \frac{1}{\mu - U'} \tanh \frac{\beta(\mu - U')}{2} \tag{9.3}$$

at large negative or positive values of μ'. The temperature T_c^0 has a meaning of maximum temperature at which the SF phase in the pure hard-core boson case disappears (in the mean-field approximation). When $\mu' < 0, \quad |\mu'| \gg U'$, the fermions are practically absent ($\overline{n}_f \approx 0$), while

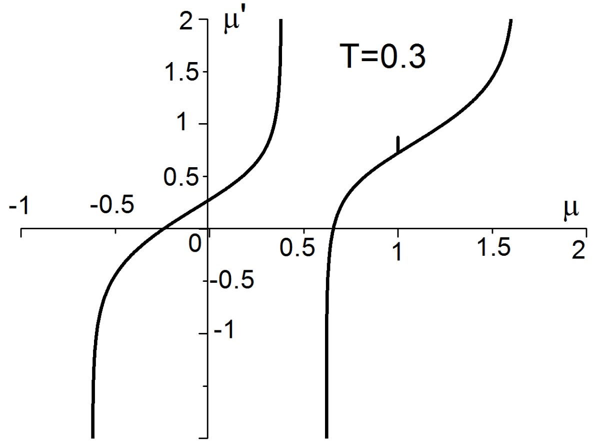

Fig.11b (μ, μ') phase diagram at $T = 0.3, |t_0| = 0.8, U' = 1$

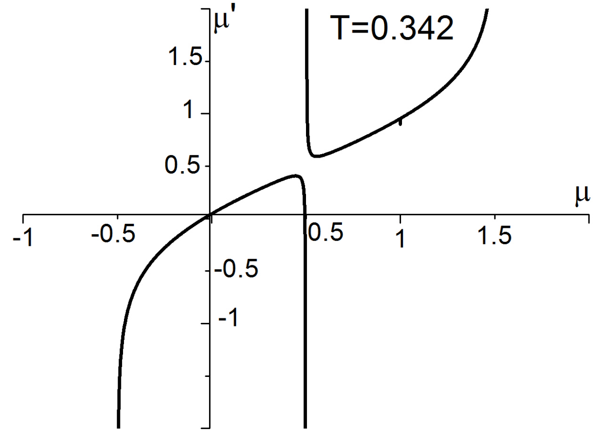

Fig.11c (μ, μ') phase diagram at $T = 0.34, |t_0| = 0.8, U' = 1$

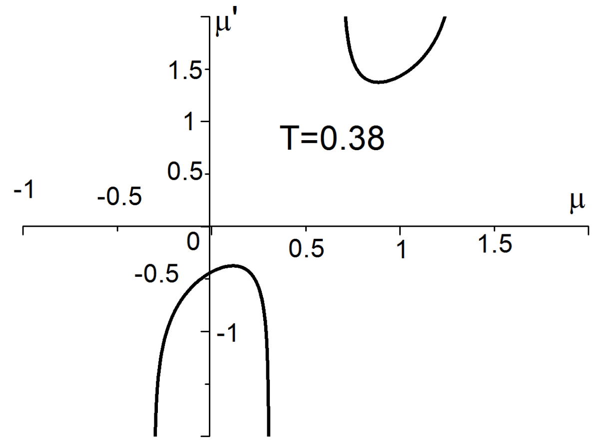

Fig.11d (μ, μ') phase diagram at $T = 0.342, |t_0| = 0.8, U' = 1$

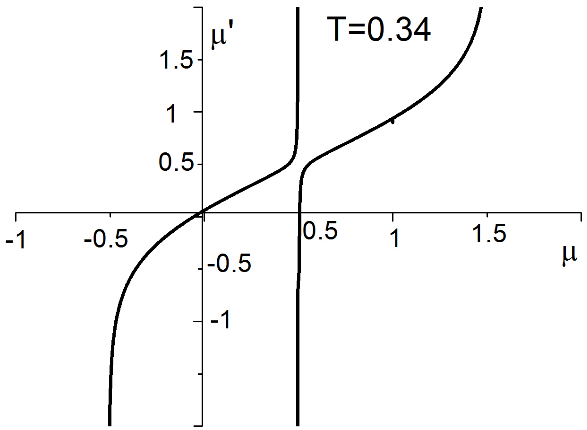

Fig.11e (μ, μ') phase diagram at $T = 0.38, |t_0| = 0.8, U' = 1$

at $\mu' > 0, \quad |\mu'| \gg U'$ the almost all lattice sites are occupied by fermions ($\overline{n}_f \approx 1$). In both limits the fermions have no influence on phase transition in boson subsystem shifting only the critical value of the boson chemical potential. Phase transitions curves in the (T, μ) plane have a form of domes, which are symmetrical with respect to $\mu = 0$ or $\mu = U'$ points (where the maxima of domes are located).

10. The $\mu = U'/2$ case

The symmetric case when $\mu = U'/2$ (corresponding to the half-filling of bosons ($\overline{n}_B = 1/2$)) is worth of separate investigation. Consideration of thermodynamics of the model greatly simplifies here.

The energies of local states (3.8) in such a case are:

$$\varepsilon_{0',1'} = -\frac{U'}{4} \pm \sqrt{\left(\frac{U'}{4}\right)^2 + t_0^2\varphi^2},$$
$$\varepsilon_{\tilde{0}',\tilde{1}'} = -\mu' + \frac{U'}{4} \pm \sqrt{\left(\frac{U'}{4}\right)^2 + t_0^2\varphi^2} \tag{10.1}$$

Respectively, for partition function we have:

$$Z_0 = 2\left(e^{\frac{\beta U'}{4}} + e^{\beta\mu'}e^{\frac{-\beta U'}{4}}\right)\cosh\left(\beta\sqrt{(U'/4)^2 + t_0^2\varphi^2}\right), \tag{10.2}$$

and for equation for order parameter

$$\frac{1}{|t_0|} = \frac{\langle X^{1'1'}\rangle - \langle X^{0'0'}\rangle + \langle X^{\tilde{1}'\tilde{1}'}\rangle - \langle X^{\tilde{0}'\tilde{0}'}\rangle}{2\sqrt{(U'/4)^2 + t_0^2\varphi^2}} = \tag{10.3}$$
$$\frac{\sinh\left(\beta\sqrt{(U'/4)^2 + t_0^2\varphi^2}\right)}{\sqrt{(U'/4)^2 + t_0^2\varphi^2}}\,\frac{\left(e^{\frac{\beta U'}{4}} + e^{\beta\mu'}e^{\frac{-\beta U'}{4}}\right)}{Z_0}$$

After substitution the expression (10.2) we obtain the following equation

$$\sqrt{(U'/4)^2 + t_0^2\varphi^2} = \frac{|t_0|}{2}\tanh\left(\beta\sqrt{(U'/4)^2 + t_0^2\varphi^2}\right) \tag{10.4}$$

using this equation, the non-zero solution for φ can be found.

The behaviour of radical $\sqrt{(U'/4)^2 + t_0^2\varphi^2} \equiv Q$ as function of temperature is shown graphically in figure 12. The curve for Q does not reach the zero with the temperature $\theta = 1/\beta$ increase and terminates at the $Q_{min} = U'/4$ value, which corresponds to the point; at which the φ parameter goes to zero. Starting from this we can make two conclusions:

1. Non-zero solutions for φ exist only when $Q_{min} < \frac{|t_0|}{2}$, i.e. when $|t_0| > U'/2$.

2. The value $Q = Q_{min}$ corresponds to the spinodal temperature which is determined by the equation

$$U'/4 = \frac{|t_0|}{2}\tanh\beta U'/4 \tag{10.5}$$

(it follows from (10.4) when $\varphi = 0$). This leads to expression

$$\Theta_{spinod.} = \frac{U'/4}{Arth\frac{U'}{2|t_0|}} \tag{10.6}$$

From equation (10.4) and from figure 11 one can see that order parameter φ is a gradually decreasing function of temperature, which tends to zero when $\Theta \to \Theta_{spinod.}$

It is important to stress, that the order parameter φ and temperature θ_c do not depend on chemical potential of fermions μ'. It holds true for whole region of the μ' values (not only for the $0 < \mu' < U'$ interval, but also for $\mu' < 0$ and $\mu' > U'$). In considered case, the fermion subsystem has an affect on temperature of transition to the state with BEC only through interaction U' with bosons.

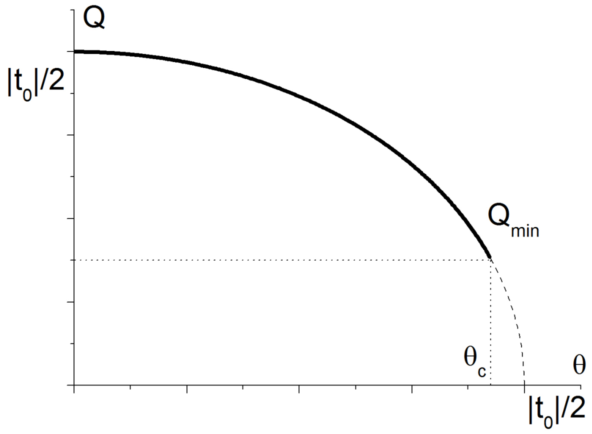

Fig.12 Radical Q as function of temperature Θ

Here, the critical value $U'_{crit} = 2|t_0|$ exists. When U' exceeds such a value, SF phase in symmetrical case $\mu = U'/2$ disappears.

The foregoing shows that at the temperature $\theta_{spinod.}$ is the same as that one, at which the SF phase region splits into two separate parts (such an effect was discussed above).

The phase transition to SF phase, taking place at $T_c = T_{spinod.}$, in this case, is of the second order.

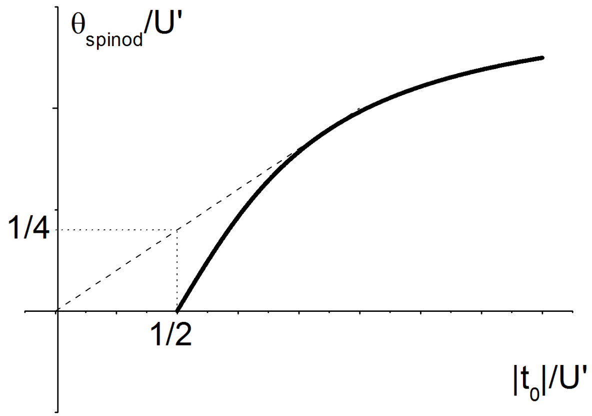

Fig.13 The temperature $\theta_{spinod.}$ as function of $|t_0|$. Dotted line corresponds to the temperature Θ_c^0

11. Conclusions

We used the Bose-Fermi-Hubbard model in the mean-field and hard-core boson approximations, in the case of infinitely small fermion transfer and repulsive on-site boson-fermion interaction, to describe phase transitions in the boson-fermion mixtures in optical lattices. Our aim was to study the conditions, at which the MI-SF transition in such a model occurs, in the case when the fermion hopping between lattice sites can be neglected. Approach used in this work does not apply the traditional scheme of mean-field approximation based on the decoupling of the on-site interaction $U'n_i^b n_i^f$. Instead of that, the Hubbard operator formalism acting on the $|n_i^b, n_i^f\rangle$ basis of states is employed; this gives a possibility to take exactly into account the boson-fermion interaction U' (the case of repulsive boson-fermion interaction ($U' > 0$) is considered in this work). The single-site problem is formulated with the only one self-consistency parameter φ ($\varphi = \langle b_i \rangle = \langle b_i^+ \rangle$), and the mean-field approach is related exclusively to description of the BE condensation.

On-site boson interaction U is treated as repulsive and infinitely large ($U > 0, U \to \infty$); that imposes restriction on occupation numbers of bosons ($n_i^b = 0$ or 1). Nevertheless, this approximation gives a possibility, as is known, to describe the MI-SF transition in the close vicinity of the $\mu = nU$ points (where n are integer numbers) in the case of finite values of U. The investigation is performed in thermodynamical regime of fixed values of chemical potentials of bosons (μ) and fermions (μ').

The equilibrium values of the order parameter φ (related to the SF phase appearing) were found from the global minimum condition of grand canonical potential Ω and, in parallel, by direct calculation of averages of creating and destroying operators of bosons $\langle b \rangle$ and $\langle b^+ \rangle$. From the obtained equation, using substitution $\varphi \to 0$, we get the condition of 2nd order phase transition to SF phase (if this transition is possible). In general, it is the condition of instability of normal (MI) phase with respect to the Bose-Einstein condensate appearance. This equation is the same as obtained earlier from the condition of divergence of the bosonic Green's function (calculated in the random phase approximation) at $\omega = 0, \mathbf{q} = \mathbf{0}$. The spinodal lines are calculated at $T = 0$ and $T \neq 0$ and corresponding phase diagrams on the (μ, μ') and (μ, T) planes are built.

For the ground state ($T = 0$) we separated 3 possible cases depending on the value of the chemical potential of fermions μ' and drew the corresponding phase diagrams where one can see the changes in the ground state. Also, the dependences of the order parameter φ and the grand canonical potential Ω on μ (at different temperatures and chemical potential μ' values) are derived.

Considering the order parameter dependence upon chemical potential of bosons (μ) we found the in the region of intermediate values of μ' (especially at $0 \leq \mu' \leq U'$), the mixing of "tilded" and "untilded" states leads to deformation of the curve $\varphi(\mu)$. The cases are distinguished, when such a dependence has a reverse behaviour and the MI-SF phase transitions changes its order from the 2nd to the 1st one (our analysis is performed in details for the case $U'/2 < |t_0| < U'$). In particular, in the vicinity of $\mu' = 0$ and $\mu' = U'$ values the $\varphi(\mu)$ dependence has a reverse course and S-like behaviour. This is an evidence of possibility of the first order phase transition (instead of the second order one). This conclusion was confirmed by calculation of grand canonical potential $\Omega_{MF}(\mu)$ as function of μ. As a result we showed that the region of existence of SF phase at $T = 0$ is wider then the limited one by spinodals. Described above effect of the phase transition order change disappears when chemical potential μ' is placed near middle of the $[0, U']$ interval corresponding to the fractional ($0 < \overline{n}_f < 1$) fermion concentration. In particular, it takes place at $0 < \mu' \lesssim 0,35U'$ and $0,65U' \lesssim \mu' < U'$, when $|t_0| = 0,8U'$. BE condensation, taking place in this case, is influenced by states which differ by number of fermions.The point $\mu' = U'/2$ is a special one. With decrease of μ', the fragmentation of SF region on two parts takes place at this point.

The similar investigation was done in the case of non-zero temperature. Outside the $[0, U']$ interval for μ', the curves of spinodals have the usual dome-like shape. Attaining to this area, the curves undergo an appreciable deformation, and when they enter inside, the regions with two temperatures of instability, corresponding to one value of μ, appear. With the change of T the "re-entrant" transitions became possible. To get the real (T, μ) phase diagrams, we investigated the grand canonical potential behaviour in such regions. We found that at higher temperatures the reverse course of $\varphi(\mu)$ function and "fishtail" of Ω_{MF}/N gradually decrease and disappear; at some temperature, that corresponds to tricritical point, the order of phase transition changes from first to second. In almost all cases for $0 < \mu' < U'$ interval there are regions where "re-entrant" transitions take place. In these cases the SF phase exists as intermediate one between temperature regions where the normal phase is stable.

We also considered the phase diagrams (μ, μ') at nonzero temperatures. In the region of temperatures above the tricritical ones (which reach a maximum of the order of $0,075U'$) the phase transition lines

coincide with spinodales; the transitions, as such, are of the 2nd order. In the case $U'/2 < |t_0| < U'$, there is observed the change of shape of the SF phase region during gradual raising of temperature, starting from $\Theta = 0,1U'$. At certain (critical) temperature Θ_c the change of topology of phase diagrams occurs. The SF phase region becomes biconnected and such a splitting into two parts is realized at point with coordinates $\mu = \mu' = 0,5U'$. For these values of chemical potentials we have at $\Theta = \Theta_c$ the second order phase transition from the SF to MI phase. At the further increase of temperature the separated SF phase regions move away one from another and become narrower.

We also investigate the symmetric case $\mu = U'/2$ (which corresponds to the boson half-filling ($\overline{n}_B = 1/2$). Consideration of thermodynamics of the model greatly simplifies here. The order parameter φ and temperature Θ_c do not depend on chemical potential of fermions μ' in this case. The fermion subsystem has an effect on temperature of transition to the state with BEC only through interaction U' with bosons. Here, the critical value $U'_{crit} = 2|t_0|$ exists. When U' exceeds such a value, SF phase in symmetrical case $\mu = U'/2$ disappears.

References

1. M. Greiner, O. Mandel, T.Esslinger, T.E. Hänsch, and I.Bloch, Nature (London) 415, 39 (2002).
2. M. Greiner, C.A. Regal, and D.S. Jin, Nature (London), 426, 537 (2003).
3. M.P.A. Fisher, P.B. Weichman, G. Grinstein, and D.S. Fisher, Phys. Rev. B40, 546 (1989).
4. D. Jaksch, C. Bruder, J.I. Cirac, C.W. Gardiner, and P. Zoller, Phys. Rev. Lett. 81, 3108 (1998).
5. D. van Oosten, P.van der Straten, and H.T.C. Stoof, Phys. Rev., A63, 053601 (2001).
6. N. Elstner and H. Monien, Phys. Rev., B59, 012184 (1999).
7. G.G. Batrouni, R.T. Scalettar, and G.T. Zimanyi, Phys. Rev. Lett. 65, 1765 (1990).
8. S.R. Clark and D. Jaksch, New J. Phys., 8, 160 (2006).
9. D.B.M. Dirkerscheid, D. van Oosten, P.J.H. Denteneer, and H.T.C. Stoof, Phys. Rev., A68, 043623 (2006).
10. K. Sengupta and N. Dupuis, Phys.Rev., A71, 033629 (2005).
11. Y. Ohashi, M. Kitaura, and H. Matsumoto, Phys. Rev., A73, 033617 (2006).

12. S.D. Huber, E. Altman, H.P. Büchler, and G. Blatter, Phys. Rev. B 75, 085106 (2007)
13. S. Konabe, T. Nikuni, and M. Nakamura, Phys. Rev., A73, 033621 (2006).
14. I.V. Stasyuk and T.S. Mysakovych, Condens Matter Phys., 12, 539 (2009).
15. I. Bloch, Nature Phys., 1, 23 (2005).
16. I. Bloch, J. Dalibard, and W. Zwerger, Rev. Mod. Phys., 80, 885 (2008).
17. M. Lewensteine, A. Sanpera, and V. Ahufinger, Ultracold atoms in opti- cal lattices: Simulating quantum many-body systems, Oxford University Press, 2012–496 pp.
18. T. Best, S.Will, U. Schneider, L. Hackenmüller, D. van Oosten, I. Bloch, and D.-S. Lühmann, Phys. Rev. Lett.,102, 030408 (2009).
19. K. Gunter, T. Stoferle, H. Moritz, M. Kohl, and T. Essling, Phys. Rev. Lett., 96, 180402.
20. C. Ospelkans, S. Ospelkans, L. Humbert, P. Ernst, K. Sengst, and K. Bongs, Phys. Rev. Lett., 97, 120402 (2006).
21. D.-S. Lühmann, K. Bongs, K. Sengstock, and D. Pfannkuche, Phys. Rev. Lett., 101, 050402 (2008).
22. S. Tewari, R.M. Lutchyn, and S. Das Sarma, Phys. Rev. B80, 054511 (2009).
23. A. Mering and M. Fleischhauer, Phys. Rev., A77, 023601 (2008).
24. O. Jürgensen, K. Sengstock, and Dirk-Sören Lühmann, Phys. Rev. A 86, 043623 (2012)
25. M. Bukov and L. Pollet, Phys. Rev. B 89, 094502 (2014) 2014.
26. H. Fehrmann, M. Baranov, M. Lewenstein, and L. Santos, Optics. Ex- press, 12, 55 (2004).
27. M. Cramer, J. Eisert, and F. Illuminati, Phys. Rev. Lett. 93, 190405 (2004)
28. H. Feshbach, Ann. Phys. 5, 337 (1958).
29. S. Inouye, M.R. Andrews, J. Stenger, H.-J. Miesner, D.M.Stamper-Kurn, and W. Ketterle, Nature, 392, 151 (1998).
30. A. Albus, F. Illuminati, and J. Eisert, Phys. Rev., A68, 023606.(2003)
31. H. Fehrmann, M.A. Baranov, B. Damski, M. Lewenstein and L. Santov, Optics Communications, 243, (2004)
32. M. Lewenstein, L. Santos, M.A. Baranov, and H. Fehrmann, Phys. Rev. Lett. 92, 050401 (2004)
33. H.P. Büchler and G. Blatter, Phys. Rev. Lett., 91, 130404 (2003).
34. T.P. Polak and T.K. Kopeć, Phys. Rev. A 81, 043612 (2010).

35. G. Refael and E. Demler, Phys. Rev., B77, 144511 (2008).
36. I. Titvinidze, M. Snoeck, W. Hofstetter, Phys. Rev. Lett. 100, 100401 (2008)
37. P. Anders, P. Werner, M. Troyer, M. Sigrist, and L. Pollet, Phys. Rev. Lett. 109, 206401 (2012)
38. M.J. Bijlsma, B.A. Herings, and H.T.C. Stoof, Phys. Rev., A61, 053601 (2000).
39. H. Heiselberg, C.J. Pethick, H. Smith, and L. Viverit, Phys. Rev. Lett., 85, 2418 (2000).
40. L. Viverit and B. Giorgini, Phys. Rev., A66, 063604 (2002).
41. R.M. Lutchyn, S. Tewari, and S. Das Sarma, Phys. Rev., A79, 011606 (2009).
42. L. Mathey, D.W. Wang, W. Hofstetter, M.D. Lukin, and E. Delmer, Phys. Rev. Lett. 93, 120404 (2004)
43. G.D. Mahan, Phys. Rev., B14, 780 (1976).
44. R. Micnas, J. Ranninger, and S. Robaszkiewicz, Rev. Mod. Phys., 62, 113 (1990).
45. K. Sengupta, N. Dupuis, and P. Majumdur, Phys. Rev., A75, 063625 (2007).
46. I.V. Stasyuk and O.V. Velychko, Condens. Matter Phys., 14, 13004 (2011).
47. I.V. Stasyuk and O. Vorobyov, Condens. Matter Phys., 16, 23005 (2013).
48. T. Mysakovych, V.O. Krasnov, and I.V. Stasyuk, Condens. Matter Phys., 11, 663 (2008).
49. T.S. Mysakovych, J. Phys.: Condens Matter, 22, 355601 (2010).
50. T.S. Mysakovych, Physica B406, 1858 (2011).
51. V.O. Krasnov, Ukr. Journ. Phys., accepted (2014).
52. A. Sanpera, A. Kantian, L. Sanchez-Palencia, J. Zakrzewski, and M. Lewenstein, Phys. Rev. Lett. 93, 040401 (2004)
53. T. Schultz et al., Acta Phys. Polon., A109, 89 (2006).
54. I.V. Stasyuk, T.S. Mysakovych, V.O. Krasnov, Condens. Matter Phys., 13, 13003 (2010).